Contribution from the Department of Pharmaceutical Sciences, Nagoya City University, Nagoya 467, Japan, and Faculty of Pharmaceutical Sciences, University of Tokyo, Tokyo 113, Japan

Imidazole Adducts of (Octaethylporphinato)iron(III) Methoxide: Resonance Raman Evidence for the Formation of Hydrogen Bonds between Sterically Hindered Imidazoles and Methoxide

Tadayuki Uno,*[1a] Keiichiro Hatano,[1a] Tatsuya Nawa,[1a] Kazuko Nakamura,[1a] Yoshifumi Nishimura,[1b,c] and Yoji Arata[1b]

Received April 9, 1991

The reactions of (octaethylporphinato)iron(III) methoxide, Fe(OEP)(OMe), with a series of imidazoles and methanol were monitored by spectrophotometric technique. One mole of Fe(OEP)(OMe) was equilibrated with 1 mol of sterically hindered imidazoles (2-RImH) or methanol to form a product. The equilibrium constant was dependent on the pK_a (BH^+) value of 2-RImH, the larger the value the smaller the pK_a. The product species were characterized by resonance Raman spectroscopy and were found to form a new class of imidazole adducts. They were five-coordinate ferric high-spin species with methoxide as the only axial ligand. The added 2-RImH forms a hydrogen bond to the methoxide ligand through its NH proton. The hydrogen bonding downshifted the ν(Fe-OMe) stretching Raman line at 541 cm^{-1} in Fe(OEP)(OMe) by ca. 20 cm^{-1} in the adduct product. The formation of these adducts suggests that the distal histidine residue itself has an ability to form a hydrogen bond spontaneously in heme proteins. On the other hand, the equilibrium reaction of Fe(OEP)(OMe) with unhindered imidazoles proceeded, as well established, in an apparent one-step process with 2 mol of imidazoles to form the six-coordinate ferric low-spin complexes. The correlation of the equilibrium constants to pK_a values of unhindered imidazoles displayed the opposite trend, the larger the value the larger the pK_a. The differences in the reactivities between the hindered and the unhindered imidazoles were discussed.

Introduction

In heme proteins such as hemoglobin, myoglobin, and peroxidases, the fifth coordination site of iron porphyrin is occupied by an imidazole from a histidine residue (proximal histidine), which is able to make a hydrogen bond through the NH moiety to influence the structure and the reactivity of the proteins.[2] A substrate molecule such as dioxygen or a peroxide ligates at the sixth coordination site of the heme iron. The ligated substrates have also been able to form hydrogen bonds from the second histidine residue locating near the sixth coordination site (distal histidine). The resonance Raman (RR)[3] and ESR spectra,[4] as well as the neutron[5] and X-ray[6] diffraction studies, have supported hydrogen bonding from the distal histidine to dioxygen in oxymyoglobin and oxyhemoglobin. In horseradish peroxidase, the presence of a distal histidine residue that affects the Fe-CO bonding in the ferrous CO complex was suggested by RR[7] and IR[7b,8] studies. This residue has been suggested to form a hydrogen bond to the oxene ligand in the peroxidase intermediate, called compound II, through which the reactivities of compound II are controlled.[9]

The importance of hydrogen bonding should also be recognized in the model studies where the reaction system is simplified by removing the protein environment. Thus far, many studies[10] have been concerned with the reactions of imidazole derivatives with iron(III) porphyrin complexes Fe(P)(X), where X denotes an exchangeable anionic ligand. It has been established that 2 mol of imidazoles are generally involved in the reaction, and bis-coordinated complexes are ultimately formed.[10] Nevertheless, few studies have been done on the reaction of the hindered imidazoles (2-RImH), which have a significant steric interaction between the substituent on the α-position of ligands and the porphyrin core as well as a comparable hydrogen-bonding potential. Though the equilibrium reaction of hindered imidazoles with Fe(PPDME)(Cl) was measured,[11] the structure of the product species has remained uncertain.

In the previous studies,[10,11] only weakly ligating anions such as Cl^- and ClO_4^- have been taken into account as the starting iron

(1) (a) Nagoya City University. (b) University of Tokyo. (c) Present address: Graduate School of Integrated Science, Yokohama City University, Seto 22-2, Kanazawa-ku, Yokohama 236, Japan.

(2) (a) Salemme, F. R.; Freer, S. T.; Xuong, N. H.; Alden, R. A.; Kraut, J. *J. Biol. Chem.* **1973**, *248*, 3910. (b) Mathews, F. S.; Czerwinski, E. W.; Argos, P. *Porphyrins* **1979**, *7*, 108. (c) Timkovich, R. *Porphyrins* **1979**, *7*, 241. (d) Wang, J. H. *Oxygenases*; Hayaishi, O., Ed.; Academic Press: New York, 1962; p 499. (e) Caughey, W. S. *Hemes and Hemoproteins*; Estabrook, R. E., Yonetani, T., Eds.; Academic Press: New York, 1966; p 285. (f) Valentine, J. S.; Sheridan, R. P.; Allen, L. C.; Kahn, P. C. *Proc. Natl. Acad. Sci. U.S.A.* **1979**, *76*, 1009. (g) Teraoka, J.; Kitagawa, T. *J. Biol. Chem.* **1981**, *256*, 3969. (h) Brautigan, D. L.; Feinberg, B. A.; Hoffman, B. M.; Margoliash, E.; Peisach, J.; Blumberg, W. E. *J. Biol. Chem.* **1977**, *252*, 574. (i) Chevion, M.; Salhany, J. M.; Peisach, J.; Castillo, C. L.; Blumberg, W. E. *Isr. J. Chem.* **1977**, *15*, 311. (j) Stanford, M. A.; Swartz, J. C.; Phillips, T. E.; Hoffman, B. M. *J. Am. Chem. Soc.* **1980**, *102*, 4492. (k) La Mar, G. N.; de Ropp, J. S.; Chacko, V. P.; Satterlee, J. D.; Erman, J. S. *Biochim. Biophys. Acta* **1982**, *708*, 317.

(3) Abbreviations used: RR, resonance Raman; ImH, imidazole; 2-MeImH, 2-methylimidazole, 2-EtImH, 2-ethylimidazole; 2-PhImH, 2-phenylimidazole; BzImH, benzimidazole; 1,2-Me_2Im, 1,2-dimethylimidazole; 4-MeImH, 4-methylimidazole; 1-MeIm, 1-methylimidazole, py, pyridine; 4-Mepy, 4-methylpyridine, 3,4-Me_2py, 3,4-dimethylpyridine; 4-Me_2Npy, 4-(dimethylamino)pyridine; OEP, dianion of octaethylporphyrin; TPP, dianion of tetraphenylporphyrin; PPDME, dianion of protoporphyrin dimethyl ester; DPDME, dianion of deuteroporphyrin dimethyl ester; X^-, generalized notation for anionic ligand.

(4) (a) Ikeda-Saito, M.; Iizuka, T.; Yamamoto, H.; Kayne, F. J.; Yonetani, T. *J. Biol. Chem.* **1977**, *252*, 4882. (b) Ikeda-Saito, M.; Brunori, M.; Yonetani, T. *Biochim. Biophys. Acta* **1978**, *533*, 173. (c) Kitagawa, T.; Ondrias, M. R.; Rousseau, D. L.; Ikeda-Saito, M.; Yonetani, T. *Nature (London)* **1982**, *298*, 869.

(5) Phillips, S. E. V.; Schoenborn, B. P. *Nature (London)* **1981**, *292*, 81.

(6) Shaanan, B. *Nature (London)* **1982**, *296*, 683.

(7) (a) Evangelista-Kirkup, R.; Smulevich, G.; Spiro, T. G. *Biochemistry* **1986**, *25*, 4420. (b) Uno, T.; Nishimura, Y.; Tsuboi, M.; Makino, R.; Iizuka, T.; Ishimura, Y. *J. Biol. Chem.* **1987**, *262*, 4549.

(8) (a) Barlow, C. H.; Ohlsson, P.-I.; Paul, K.-G. *Biochemistry* **1976**, *15*, 2225. (b) Smith, M. L.; Ohlsson, P.-I.; Paul, K. G. *FEBS Lett.* **1983**, *163*, 303. (c) Smith, M. L.; Paul, J.; Ohlsson, P. I.; Paul, K. G. *Biochemistry* **1984**, *23*, 6776.

(9) (a) Makino, R.; Uno, T.; Nishimura, Y.; Iizuka, T.; Tsuboi, M.; Ishimura, Y. *J. Biol. Chem.* **1986**, *261*, 8376. (b) Sitter, A. J.; Reczek, C. M.; Terner, J. *J. Biol. Chem.* **1985**, *260*, 7515. (c) Sitter, A. J.; Shiflett, J. R.; Terner, J. *J. Biol. Chem.* **1988**, *263*, 13032. (d) Hashimoto, S.; Tatsuno, Y.; Kitagawa, T. *Proc. Natl. Acad. Sci. U.S.A.* **1986**, *83*, 2417.

(10) (a) Coyle, C. L.; Rafson, P. A.; Abbot, E. H. *Inorg. Chem.* **1973**, *12*, 2007. (b) Abbot, E. H.; Rafson, P. A. *J. Am. Chem. Soc.* **1974**, *96*, 7378. (c) Walker, F. A.; Lo, M.-W.; Ree, M. T. *J. Am. Chem. Soc.* **1976**, *98*, 5552. (d) Nappa, M.; Valentine, J. S.; Snyder, P. A. *J. Am. Chem. Soc.* **1977**, *99*, 5799. (e) Pasternack, R. F.; Stahlbush, J. R. *J. Chem. Soc., Chem. Commun.* **1977**, 106. (f) Pasternack, R. F.; Gillies, B. S.; Stahlbush, J. R. *J. Am. Chem. Soc.* **1978**, *100*, 2613. (g) Wang, J.-T.; Yeh, H. J. C.; Johnson, D. F. *J. Am. Chem. Soc.* **1978**, *100*, 2400. (h) La Mar, G. N.; Walker, F. A. *J. Am. Chem. Soc.* **1972**, *94*, 807. (i) La Mar, G. N.; Satterlee, J. D.; Snyder, R. V. *J. Am. Chem. Soc.* **1974**, *96*, 7137. (j) Satterlee, J. D.; La Mar, G. N.; Frye, J. S. *J. Am. Chem. Soc.* **1976**, *98*, 7275. (k) Satterlee, J. D.; La Mar, G. N.; Bold, T. J. *J. Am. Chem. Soc.* **1977**, *99*, 1088.

(11) Yoshimura, T.; Ozaki, T. *Bull. Chem. Soc. Jpn.* **1977**, *52*, 2268.

0020-1669/91/1330-4322$02.50/0

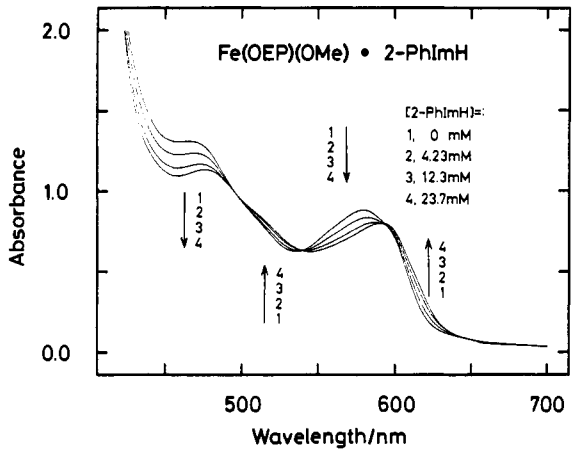

Figure 1. Visible spectral changes upon addition of 2-PhImH to Fe(OEP)(OMe). Aliquots of 2-PhImH solutions were added to Fe(OEP)(OMe) in methylene chloride. Concentrations of 2-PhImH (mM): (1) 0; (2) 4.23; (3) 12.3; (4) 23.7.

porphyrin species. On the other hand, alkoxide belongs to another class of ligands having a high affinity to iron(III) porphyrinate. In this work, we utilized RR spectroscopy to characterize the product species when Fe(OEP)(OMe) was reacted with 2-RImH and established that a new class of imidazole adducts is formed. The vibrational frequencies of the RR spectra have revealed that 2-RImH does not coordinate directly to the iron atom at the initial stage, but forms a hydrogen bond from the NH proton of the 2-RImH moiety to the methoxide ligand. This suggests that the distal histidyl imidazole in heme proteins spontaneously forms a stable adduct with the iron ligand through the hydrogen-bonding interaction and may give a clue to understanding the role of distal histidine in controlling the heme reactivity.

Materials and Methods

Spectrophotometric Measurements. The crystalline Fe(OEP)(Cl) (Aldrich) and Fe(OEP)(OMe) were prepared as described.[12] ImH, 2-MeImH, BzImH, and 4-Me_2Npy were recrystallized from benzene. 2-PhImH was recrystallized from chloroform/petroleum ether. Spectrophotometric measurements were made on a Shimadzu UV-2100 spectrophotometer. Equilibrium constants were determined from the absorbance changes of ca. 0.1 mM Fe(OEP)(OMe) or Fe(OEP)(Cl) dissolved in methylene chloride (Nakarai Chemicals, SP Grade) to which aliquots of imidazole or pyridine stock solutions were added. The Fe(OEP)(OMe) was also titrated with CH_3OH (Nakarai Chemicals, SP Grade) and CH_3OD (99.5 atom % D, Aldrich). The procedure for obtaining the equilibrium constants is given elsewhere.[13]

RR Spectroscopy. RR spectra were measured by using a detecting system as described previously.[7b,9a] The spectra in Figure 3A,B were obtained by the use of a photomultiplier (Hamamatsu Photonics, R-585), while others were obtained on a Tracor Northern IDARSS system. The data acquisition time for the detection by the latter system was 200 s for each spectrum.

(12) Hatano, K.; Uno, T. *Bull. Chem. Soc. Jpn.* **1990**, *63*, 1825.
(13) Uno, T.; Hatano, K.; Nishimura, Y.; Arata, Y. *Inorg. Chem.* **1990**, *29*, 2803. The equilibrium reaction of Fe(OEP)(X) with n mol of ligand (L) is expressed as

$$\mathrm{Fe(OEP)(X)} + n\mathrm{L} \rightleftharpoons \mathrm{Fe(OEP)(L)}_n\mathrm{X}$$

$$K = [\mathrm{Fe(OEP)(L)}_n\mathrm{X}]/[\mathrm{Fe(OEP)(X)}][\mathrm{L}]^n$$

where K is the equilibrium constant. The initial concentration of Fe(OEP)(X), $[\mathrm{Fe(OEP)(X)}]_0$, is expressed as

$$[\mathrm{Fe(OEP)(X)}]_0 = [\mathrm{Fe(OEP)(L)}_n\mathrm{X}] + [\mathrm{Fe(OEP)(X)}]$$

Thus we obtain

$$K = \frac{[\mathrm{Fe(OEP)(X)}]_0 - [\mathrm{Fe(OEP)(X)}]}{[\mathrm{Fe(OEP)(X)}][\mathrm{L}]^n}$$

The logarithm of the above equation, after rearrangement, gives

$$-\log\left(\frac{[\mathrm{Fe(OEP)(X)}]_0}{[\mathrm{Fe(OEP)(X)}]} - 1\right) = -\log K - n\log[\mathrm{L}]$$

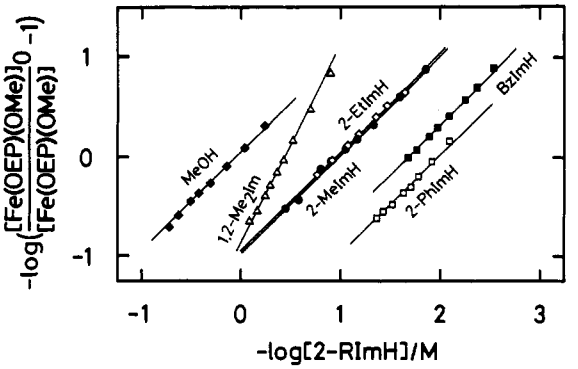

Figure 2. Graphical method for analysis of absorbance data for the reactions of sterically hindered imidazole derivatives and methanols with Fe(OEP)(OMe).

Table I. log K Values for Addition of 2-RImH and the Spectrophotometric Data, along with the ν(Fe–OMe) Stretching Frequency

2-RImH	$pK_a(BH^+)$	log K	band I/nm	ν(Fe–OMe)/cm^{-1}
BzImH	5.53	1.66 ± 0.02[a]	592	516
2-PhImH	6.09	1.97 ± 0.03	593	517 (−14)[b]
2-MeImH	7.56	0.96 ± 0.04	591	521
2-EtImH	7.70	0.94 ± 0.03	590	522
CH_3OH		−0.06 ± 0.03	592	527
CH_3OD		−0.08 ± 0.03	591	540 (−13)
none			580	541 (−10)

[a] Equilibrium constants (K in M^{-1}) were determined in CH_2Cl_2 solvent. [b] Values in parentheses are the isotope shift by perdeuterated methanol.

The 406.7-nm line of a krypton ion laser (Spectra Physics, SP 164-01) was employed as an excitation source. Laser power at the sample was approximately 10 mW. A methylene chloride solution containing ca. 0.1 mM Fe(OEP)(OMe) and an appropriate amount of imidazole derivative or methanol (CH_3OH, CH_3OD) was prepared. Perdeuterated methanol (CD_3OD, 99 atom % D, from Merck) was used for the isotope shift experiments. The sample was spun in the rotating cell throughout the measurements to avoid local heating and to minimize the photoinduced decomposition.

Results

Equilibrium Reaction of Hindered Imidazoles (2-RImH) and Methanol with Fe(OEP)(OMe). In Figure 1 are shown the typical spectral changes that take place in the visible region when 2-PhImH was added to Fe(OEP)(OMe). Isosbestic points are clearly observed, indicating that the transition is composed of two spectral species in equilibrium. The absorption maxima of the Fe(OEP)(OMe) complex, which were observed at 467 and 580 nm,[13] are replaced by new peaks at about 480 nm (band IV)[14] and 590 nm (band I).

The reaction was consistent with the following expression involving 1 mol of 2-RImH and the adduct product:

$$\mathrm{Fe(OEP)(OMe)} + \text{2-RImH} \overset{K}{\rightleftharpoons} \mathrm{Fe(OEP)(OMe)}\cdot\text{2-RImH}$$

$$K = \frac{[\mathrm{Fe(OEP)(OMe)}\cdot\text{2-RImH}]}{[\mathrm{Fe(OEP)(OMe)}][\text{2-RImH}]}$$

The values of log K obtained graphically[13] (Figure 2) are summarized in Table I, along with the absorption maxima (band I) of the product species. It is clear that an acidic imidazole derivative (small pK_a value) gives a large log K value and that the band I is commonly located at about 590 nm.

Addition of methanol to Fe(OEP)(OMe) gave similar spectral changes proceeding with one set of isosbestic points, and the reaction was well analyzed as analogous to that of hindered imidazoles (Figure 2). The equilibrium constant values for addition

(14) Falk, J. E. *Porphyrins and Metalloporphyrins*; Elsevier: Amsterdam, 1964.

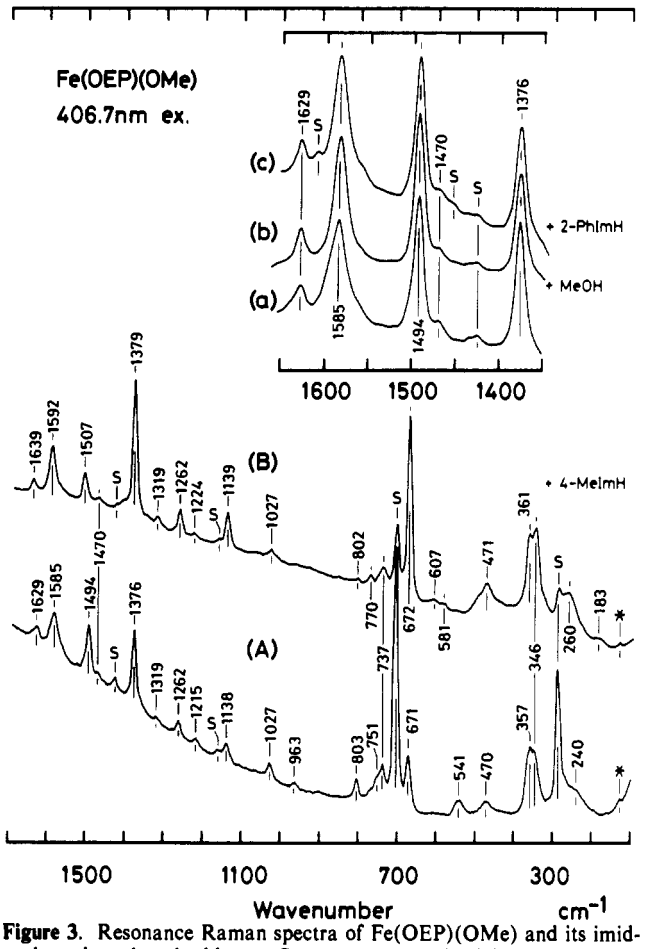

Figure 3. Resonance Raman spectra of Fe(OEP)(OMe) and its imidazole and methanol adducts. Spectra were obtained for ca. 0.15 mM Fe(OEP)(OMe) dissolved in methylene chloride with (A) 0.31 M methanol, (B) 0.33 M 4-MeImH, (a) 0.31 M methanol, (b) 5.2 M methanol, and (c) 48 mM 2-PhImH and 0.31 M methanol. The lines marked with S and an asterisk denote those of the solvent and the natural emission from the laser, respectively. Raman scattering was excited with the 406.7-nm line. Slit width: 5 cm^{-1}.

of CH_3OH and CH_3OD were essentially the same (Table I).

RR Spectra. The RR spectrum of Fe(OEP)(OMe) is shown in Figure 3A. Since Fe(OEP)(OMe) was found to decompose slowly during the RR measurement, the RR spectra of Fe(OEP)(OMe) were obtained in the presence of 1.25% (v/v) methanol (0.31 M). Under these conditions, the undesired methanol adduct, Fe(OEP)(OMe)·MeOH, was present at about a 20% level, as estimated from the equilibrium constant (Table I), and therefore the disturbance by this species of the RR spectra of Fe(OEP)(OMe) was less pronounced (cf. Figure 4A,D).

Structural information about the Fe(OEP) moiety can be obtained by evaluating RR frequencies of several OEP vibrations that are sensitive to the changes in the oxidation, spin, and coordination states.[15] mn the high-frequency region, the ν_{10}, ν_2, ν_3, and ν_4 lines[16] were observed at 1629, 1585, 1494, and 1376 cm^{-1}, respectively. The high-frequency RR spectra of the reaction products, Fe(OEP)(OMe)·2-PhImH and Fe(OEP)(OMe)·MeOH, were compared with the spectrum of Fe(OEP)(OMe) as shown in the inset of Figure 3 (c, b, and a, respectively). All RR features were in perfect agreement in this region. The frequencies of the observed lines, as well as the comparison with those of Fe(OEP)(OC_6H_5) and Fe(OEP)(SC_6H_5),[13] agreed quite well with those of the five-coordinate ferric high-spin complexes.[15]

(15) (a) Spiro, T. G. *Iron Porphyrins*; Lever, A. B. P.; Gray, H. B., Eds.; Addison-Wesley: Reading, MA, 1983; Part II, p 89. (b) Spiro, T. G. *Adv. Protein Chem.* **1985**, *37*, 111. (c) Asher, S. A. *Methods Enzymol.* **1981**, *76*, 371. (d) Felton, R. H.; Yu, N.-T. *Porphyrins* **1978**, *3*, 347.
(16) Abe, M.; Kitagawa, T.; Kyogoku, Y. *J. Chem. Phys.* *1978*, *69*, 4526.

Table II. log β_2 Values for the Addition of 1-RIm and 4-RImH and the Spectrophotometric Data for the Products[a]

porphyrin	base	$pK_a(BH^+)$	log β_2	band IV/nm
Fe(OEP)(OMe)	4-Mepy	6.02	−0.75 ± 0.06	518
	3,4-Me_2py	6.46	0.64 ± 0.05	520
	ImH	6.65	3.25 ± 0.05	532
	4-MeImH	7.22	3.10 ± 0.06	528
	1-MeIm	7.33	0.83 ± 0.08	524
	1,2-Me_2Im	7.85	0.87 ± 0.05	524
	4-Me_2Npy	9.70	1.96 ± 0.09	527
Fe(OEP)(Cl)	ImH	6.65	6.02 ± 0.03	532
	4-MeImH	7.22	5.85 ± 0.08	528

[a] β_2 is in units of M^{-2}.

In the lower frequency region of the RR spectrum of Fe(OEP)(OCH_3), a Raman line at 541 cm^{-1} is prominent (Figure 3A). In the left panel of Figure 4 are shown the effects of the addition of a small amount (1.25% v/v) of methanol isotopes on the 541-cm^{-1} line. This line was found to downshift by about 10 cm^{-1} in the presence of CD_3OD (Figure 4C). This indicates that the methoxide ligand in Fe(OEP)(OCH_3) exchanges with the bulk methanol (CD_3OD) to form the Fe(OEP)(OCD_3) complex. The magnitude of the observed isotopic shift agreed with that calculated for a stretching mode of the Fe–OCH_3 molecule (−16 cm^{-1}). The 541-cm^{-1} line did not shift in the presence of CH_3OD (Figure 4B). This is consistent with methoxide anion as the ligand, but not a methanol molecule. The IR absorption that is assignable to the ν(Fe–OCH_3) stretch has been located at 542 and 540 cm^{-1} in a KBr pellet of crystalline Fe(OEP)(OCH_3)[12] and Fe(DPDME)(OCH_3),[17] respectively.

The low-frequency RR spectrum of Fe(OEP)(OCH_3)·CH_3OH which is formed at high methanol concentration (21% v/v) is shown in the right panel of Figure 4 along with deuterium substitution effects. The behavior of the ν(Fe–OCH_3) stretching line differed markedly in the presence of low vs high concentrations of methanol isotopes. A Raman line at 527 cm^{-1} is apparent in the presence of 5.2 M CH_3OH (Figure 4D). Although the frequency is lower than that observed in Fe(OEP)(OCH_3) by 14 cm^{-1} (Figure 4A), we assigned this line to the ν(Fe–OCH_3) stretching mode shifted by the adduct formation. In the presence of CD_3OD, this line was also detected at 527 cm^{-1} (Figure 4F). The downshift was less pronounced upon substitution by CH_3OD (Figure 4E), though the product species, Fe(OEP)(OCH_3)·CH_3OD, should be formed at an 80% level from the equilibrium estimation.

In the left panel of Figure 5 are shown the RR spectra in the lower frequency region when 2-PhImH was added to Fe(OEP)(OCH_3). Two Raman lines that were sensitive to the isotope substitution of methanol were observed at 541 and 517 cm^{-1}. The weaker line at 541 cm^{-1} downshifted to about 530 cm^{-1} in the presence of dilute CD_3OD and is attributable to unreacted Fe(OEP)(OCH_3). The stronger line at 517 cm^{-1} downshifted to 503 cm^{-1} by CD_3OD (Figure 5C) and is assigned to the adduct Fe(OEP)(OCD_3)·2-PhImH.

In the right panel of Figure 5, the effect of other hindered imidazoles on the ν(Fe–OMe) stretching frequency is shown. The BzImH, 2-MeImH, and 2-EtImH adducts of Fe(OEP)(OMe) are calculated to be present at 81, 66, and 81%, respectively, on the bases of equilibrium constants. A Raman line was observed at about 520 cm^{-1} in all adducts, which can be assigned to the ν(Fe–OMe) stretching mode. Therefore, the addition of 2-RImH derivatives commonly downshifted the ν(Fe–OMe) stretching frequency and hence weakened the Fe–OMe bonding. It should be noted that the ν(Fe–OMe) stretching line could not be detected in the case of 1,2-Me_2Im.

Equilibrium Reaction of Unhindered Imidazoles. Spectral changes on addition of unhindered imidazoles to Fe(OEP)(OMe) were measured in order to compare their reactivities with those of 2-RImH derivatives. Overall spectral changes were approx-

(17) Sadasivan, N.; Eberspaecher, H. I.; Fuchsman, W. H.; Caughey, W. S. *Biochemistry* **1969**, *8*, 534.

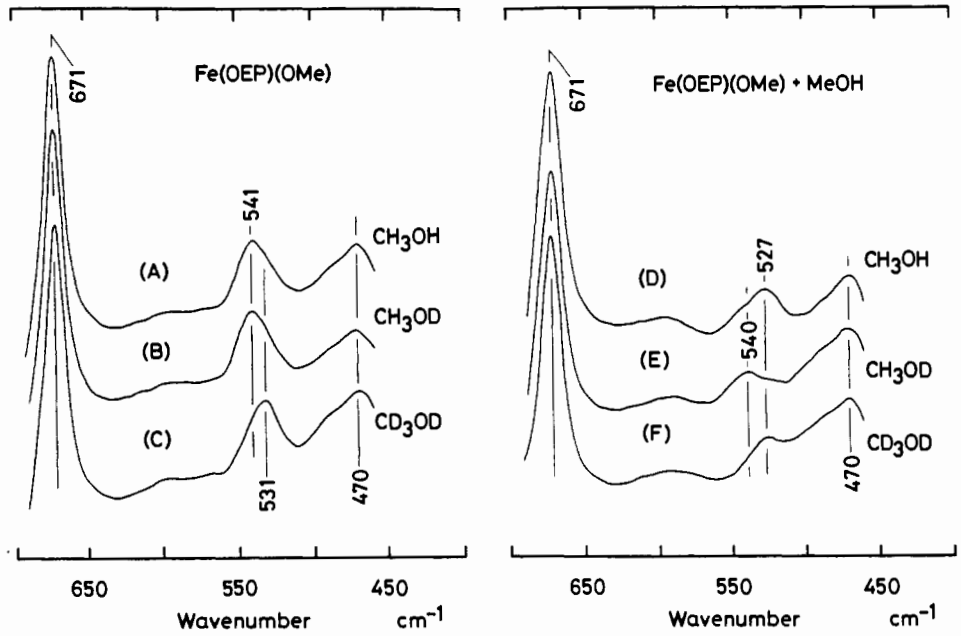

Figure 4. Effect of methanol isotopes on the resonance Raman spectrum of Fe(OEP)(OMe). Solutions of ca. 0.15 mM Fe(OEP)(OMe) dissolved in methylene chloride, which contained 0.31 M (left panel) or 5.2 M (right panel) CH_3OH (A and D), CH_3OD (B and E), and CD_3OD (C and F), were measured. Spectral conditions were the same as in Figure 3.

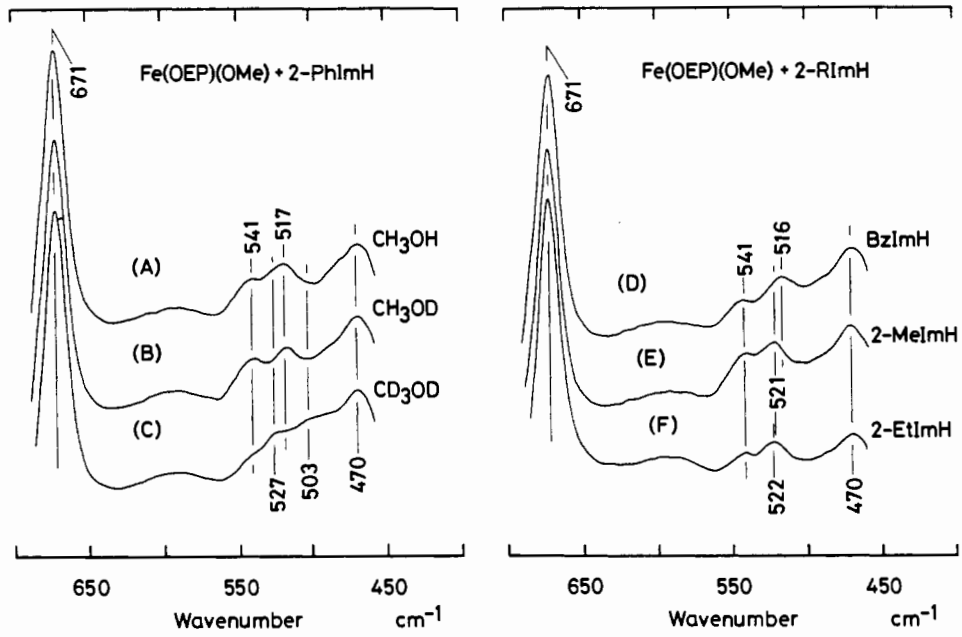

Figure 5. Effect of addition of 2-RImH on the resonance Raman spectrum of Fe(OEP)(OMe). The sample solutions contained ca. 0.15 mM Fe(OEP)(OMe) in methylene chloride, with 48 mM 2-PhImH and 0.31 M CH_3OH (A), CH_3OD (B), or CD_3OD (C) or with 0.31 M CH_3OH and 95 mM BzImH (D), 210 mM 2-MeImH (E), or 500 mM 2-EtImH (F). Spectral conditions were the same as in Figure 3.

imately analyzed[10c] via an apparent one-step reaction involving 2 mol of bases (B):

$$\mathrm{Fe(OEP)(OMe)} + 2\mathrm{B} \overset{\beta_2}{\rightleftharpoons} \mathrm{Fe(OEP)(B)_2OMe}$$

$$\beta_2 = \frac{[\mathrm{Fe(OEP)(B)_2OMe}]}{[\mathrm{Fe(OEP)(OMe)}][\mathrm{B}]^2}$$

The log β_2 values were obtained graphically[13] (Figure 6) and are summarized in Table II, along with the pK_a (BH^+) values of the bases and the wavelength maxima of band IV (around 530 nm) of the product species. We have also compared the equilibrium reaction of Fe(OEP)(Cl) with ImH and 4-MeImH (4-RImH). The log β_2 values were larger for addition to Fe(OEP)(Cl) than to Fe(OEP)(OMe) by about 2.8 log units for both ImH and 4-MeImH. This indicates that Cl^- complex dissociated more readily than Fe(OEP)(OMe).

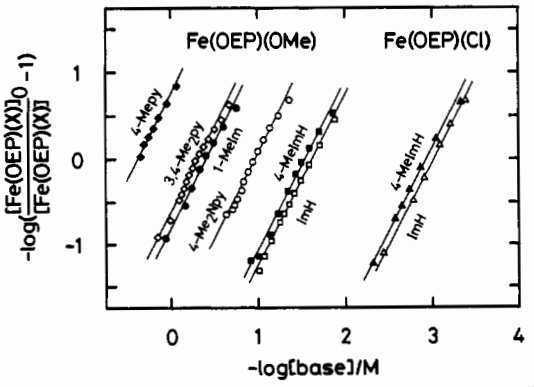

Figure 6. Graphical method for analysis of absorbance data for the reactions of unhindered imidazole and pyridine derivatives with Fe(OEP)(OMe) and Fe(OEP)(Cl).

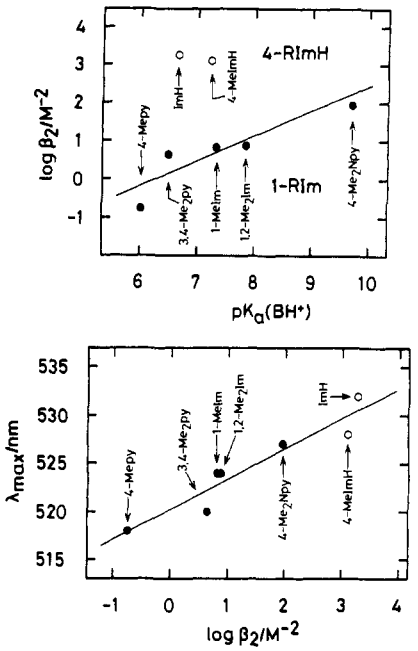

Figure 7. Correlation between pK_a values of bases and log β_2 values (upper) and between log β_2 values and absorption maxima of band IV of the product species (lower).

In Figure 3B is shown the RR spectrum of the product species when 4-MeImH was added to Fe(OEP)(OMe). The ν_{10}, ν_2, ν_3, and ν_4 modes are observed at 1639, 1592, 1507, and 1379 cm^{-1}. These frequencies were similar to those reported previously for other unhindered imidazole adducts, $[Fe(OEP)(1\text{-MeIm})_2]^+$[18] and $[Fe(OEP)(ImH)_2]^+$.[19] This indicates that the product species is the six-coordinate ferric low-spin complex[15] $[Fe(OEP)(4\text{-MeImH})_2]^+$. Both of the absorption spectra (Table II) and the RR spectra coincided completely between the products when 4-RImH was added to Fe(OEP)(Cl) and Fe(OEP)(OMe), indicating that the products were identical irrespective of the starting complexes.

In Figure 7 (upper), the log β_2 values are plotted against the $pK_a(BH^+)$ values of the imidazole and pyridine derivatives. It is clearly seen that the bases are classified into two groups. The first group consists of pyridines and imidazoles that have no NH proton, designated as 1-RIm. In this group, the derivative with a large pK_a value gives a large log β_2 value. A similar tendency has been observed in the reaction of Fe(TPP)(Cl) with imidazoles and pyridine derivatives.[10c] One hindered derivative, 1,2-Me_2Im, could be included in this group on the basis of its reactivity with Fe(OEP)(OMe) and of the similarity of the absorption spectrum of the product species (Table II).

On the other hand, the 4-RImH derivatives considerably deviated from the correlation between the pK_a and log β_2 values for 1-RIm. For instance, although the pK_a value of 4-MeImH (7.22) is similar to that of 1-MeIm (7.33), the log β_2 value is larger by more than 2 log units (3.10 and 0.83). As shown in Figure 7 (lower), however, a linear correlation is seen between the wavelength maxima of band IV and the log β_2 values, which holds for both 1-RIm and 4-RImH. The anomalous behaviors of 4-RImH are discussed below.

Discussion

Axial Coordination State in New Adducts. The absorption spectra of the adduct products of 2-RImH and methanol commonly showed wavelength maxima at about 480 and 590 nm (Table I). The spectral profiles resemble those reported[11] for the intermediates during the course of addition of hindered imidazoles to Fe(PPDME)(Cl). We have revealed by the use of RR spectroscopy that addition of 2-RImH to Fe(OEP)(OMe) produces a new class of five-coordinate species, which are designated as Fe(OEP)(OMe)·2-RImH. Thus far, imidazole derivatives have been considered[10] to coordinate directly to the iron to form bis complexes. The present RR results unequivocally indicate, however, that 2-RImH derivatives do not coordinate to the iron but produce imidazole adducts that are five-coordinate species with weak Fe–OMe bonding.

Axial coordination of 2-RImH trans to the methoxide ligand can be refuted by other pieces of evidence. For instance, the ν(Fe–CN) stretching frequency was found to be reduced by the ligation of basic (large pK_a value) pyridine derivatives at the trans side in Fe(OEP)(CN)(py).[20] This is contrary to the present case, in which the acidic 2-RImH weakened the Fe–OMe bonding (Table I). In addition, the porphyrin skeleton should suffer from the sterical interaction of the bulky 2-R substituents of the ligands if they were coordinating directly to the iron. Such an interaction should distort the porphyrin skeleton and subsequently induce sizable frequency shifts in the high-frequency RR modes.

It was found that all the skeletal modes above 1450 cm^{-1} show a negative linear dependence on Ct–N, the center-to-pyrrole nitrogen distance of the porphyrin cavity.[15,19a] From the present RR results (Figure 3), the Ct–N distance of Fe(OEP)(OMe) is estimated to be 2.01 Å. This value is in good agreement with that from the X-ray crystallography (2.005 Å).[12] In addition, the ν(Fe–OMe) stretching frequency in Fe(OEP)(OMe) coincided with the IR[12] (KBr pellet) spectra. Therefore, it is suggested that the structure of crystalline Fe(OEP)(OMe) is essentially maintained in the CH_2Cl_2 solvent.

Hydrogen Bonding. Addition of a large amount of CH_3OH to Fe(OEP)(OCH_3) reduced the ν(Fe–OCH_3) stretching frequency by about 14 cm^{-1}, but the downshift was less pronounced in Fe(OEP)(OCH_3)·CH_3OD (right panel of Figure 4). Therefore, the hydrogen atom on the methanol hydroxyl group is responsible for the downshift of the ν(Fe–OCH_3) stretching line. This fact strongly suggests that a hydrogen bond is formed from the methanol OH to the methoxide ligand as shown below.

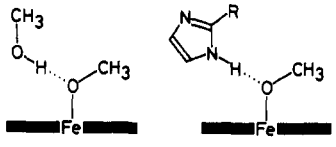

The hydrogen bonding explains the curious isotope effects of high concentration of the methanol on the RR spectra. The ν(Fe–OCH_3) stretching line at 540 cm^{-1} in Fe(OEP)(OCH_3)·CH_3OD (Fe–OCH_3···$DOCH_3$) (Figure 4E) downshifted by 13 cm^{-1} in the presence of 5.3 M CD_3OD (Fe–OCD_3···$DOCD_3$) (Figure 4F). The frequency coincided accidentally with that in Fe(OEP)-(OCH_3)·CH_3OH (Fe–OCH_3···$HOCH_3$) (Figure 4D). In other words, the mass effect of the CD_3O moiety and the hydrogen-bonding effect of OH moiety produced the same degree of downshift.

In the case of 2-RImH, the weakening of the Fe–OMe bond is also explained in terms of the formation of hydrogen bonding between the methoxide ligand and the NH moiety of 2-RImH (as shown above). The NH proton should compete with iron for a share of electron donation from the methoxide ligand toward the iron. The more acidic 2-RImH may promote the NH proton to be the more effective hydrogen bonder, and this is reflected in the lessening of ν(Fe–OMe) stretching frequency in the acidic 2-RImH adduct (Table I). This effect further explains the somewhat higher ν(Fe–OMe) stretching frequency (527 cm^{-1}) in Fe(OEP)(OMe)·MeOH than that (521 cm^{-1}) in Fe(OEP)-(OMe)·2-MeImH, since the pK_a(AH) of MeOH is ca. 15, while that of 2-MeImH is ca. 14.

As a consequence of this qualitative characterization of the hydrogen bonding, there is a possibility that such an intermediate

(18) Callahan, P. M.; Babcock, G. T. *Biochemistry* **1981**, *20*, 952.
(19) (a) Choi, S.; Spiro, T. G.; Langry, K. C.; Smith, K. M.; Budd, D. L.; La Mar, G. N. *J. Am. Chem. Soc.* **1982**, *104*, 4345. (b) Choi, S.; Spiro, T. G. *J. Am. Chem. Soc.* **1983**, *105*, 3683.
(20) Uno, T.; Hatano, K.; Nishimura, Y.; Arata, Y. *Inorg. Chem.* **1988**, *27*, 3215.

species, Fe(OEP)(OMe)·4-RImH, is formed in the course of addition of 4-RImH. It was indicated by an X-ray study[21] that fluoride ligand is hydrogen bonding with the imidazole NH moiety in $[Fe(TPP)(F)_2]^-$ isolated as the 2-MeImH$_2^+$ salt. Previous studies on the reaction kinetics of ImH with Fe(P)(X) suggested[22] that the hydrogen-bonding interaction between the imidazole NH and the departing X^- anion has a significant effect on the rate acceleration and the rate law.

The hydrogen-bonding ability of 2-RImH may be compared to that of the distal histidine residue in heme proteins. Our present results that hydrogen bonding decreases the Fe–OMe stretching vibration support the previous reports on the relation between Fe–ligand vibrations and distal histidine hydrogen bonding. In peroxidase compound II, the alkaline deprotonation of a distal amino acid group, probably histidine, has been suggested[9] to disrupt the hydrogen bonding of this group to the oxyferryl moiety, raising the $\nu(Fe^{IV}=O)$ stretching frequency. In metmyoglobin fluoride, data has been presented implicating hydrogen bonding of a ligated fluoride to the distal histidine,[23] where the ν(Fe–F) stretching frequency is lowered (461 $cm^{-1} \rightarrow$ 422 cm^{-1}) through the formation of hydrogen bonding at acidic pH.

Acid-Base Property of Imidazole Derivatives. The log β_2 value for 4-RImH was generally larger than that for 1-RIm (Figure 7, upper). A similar trend has been noted in the reactions of Fe(TPP)(Cl)[10c] and Fe(PPDME)(Cl),[11] where the log β_2 values for 4-RImH were larger than those for 1-RIm by about 3 log units on the average. This effect has been explained[10c,j,k] in terms of stabilization induced by the delocalization of the positive charge on iron(III) through the hydrogen bonding of the NH moiety of imidazole ligands. As the strength of the hydrogen bonding increases, the donor ability of the imidazole imine nitrogen also increases, resulting in more electron density on the iron. We have found a rough correlation between the basicity of 1-RIm and the value of log β_2 (Figure 7, upper); log $\beta_2 = -3.83 + 0.608[pK_a(BH^+)]$. From the log β_2 value, in turn, the pK_a value of 4-RImH is calculated to be about 11, which is ca. 4 pK_a units larger than that of free 4-RImH. This supports the suggestion[2d,e] that hydrogen bonding of the proximal histidine imidazole proton to a neighboring peptide backbone would increase the basicity of the imidazole moiety.

The equilibrium constants showed a negative correlation to the pK_a values of imidazoles in the case of 2-RImH (log K, Table I), and a positive correlation in the case of 1-RIm (log β_2, Table II). These may reflect the acid–base properties of the imidazole. We have included BzImH in the 2-RImH group on the basis of its reactivity with Fe(OEP)(OMe) (Figure 2) and of the RR spectrum of the product (Figure 5D), though it lacks a 2-R substituent. The behavior of BzImH may be understood in terms of the acid–base properties of this derivative. Since BzImH is the weakest base among the 2-RImH bases utilized in this work, BzImH is allowed to behave more readily as an acid than as a base.

Though the formation of Fe(OEP)(OMe)·2-RImH adduct is mainly attributed to the steric hindrance by the 2-R substituent, the acid–base property of 2-RImH accounts for the peculiar behavior of 1,2-Me_2Im relative to that of 2-MeImH. At low concentration, 2-MeImH behaved as an acid. Though the degree of the steric hindrance and the pK_a (BH^+) values are similar to those for 2-MeImH, 1,2-Me_2Im lacks an NH group and can behave only as a base (Figure 2).

Conclusion

The reactivities of the imidazole derivatives with Fe(OEP)(OMe) was largely dependent on the position of the substituent on the imidazole ring. Especially noted is that the 2-R substituent retarded the biscoordination of 2-RImH by a steric effect and the five-coordinated species Fe(OEP)(OMe)·2-RImH was newly produced. In this adduct, the NH proton is hydrogen bonding to the methoxide ligand and has weakened the Fe–OMe bonding. The strength of the Fe–OMe bonding was controlled by the degree of hydrogen-bonding ability of 2-RImH. This may be compared to the effect of the distal histidine in heme proteins, which has been supposed[24] to control the reactivities of the oxy ligands in hemoglobin, myoglobin, and peroxidase through the hydrogen bonding.

Acknowledgment. This work was supported, in part, by a Grant-in-aid (01771946 to T.U.) from the Ministry of Education, Science, and Culture of Japan.

Registry No. Fe(OEP)(OMe), 50652-07-8; BzImH, 51-17-2; 2-PhImH, 670-96-2; 2-MeImH, 693-98-1; 2-EtImH, 1072-62-4; CH_3OH, 67-56-1; 4-Mepy, 108-89-4; 3,4-Me_2py, 583-58-4; ImH, 288-32-4; 4-MeImH, 822-36-6; 1-MeIm, 616-47-7; 1,2-Me_2Im, 1739-84-0; 4-Me_2Npy, 1122-58-3; Fe(OEP)(Cl), 28755-93-3.

(21) Scheidt, W. R.; Lee, Y. J.; Tamai, S.; Hatano, K. *J. Am. Chem. Soc.* **1983**, *105*, 778.

(22) (a) Burdige, D.; Sweigart, D. A. *Inorg. Chim. Acta* **1978**, *28*, L131. (b) Fiske, W. W.; Sweigart, D. A. *Inorg. Chim. Acta* **1979**, *36*, L429. (c) Doeff, M. M.; Sweigart, D. A. *Inorg. Chem.* **1982**, *21*, 3699. (d) Tondreau, G. A.; Sweigart, D. A. *Inorg. Chem.* **1984**, *23*, 1060. (e) Jones, J. G.; Tondreau, G. A.; Edwards, J. O.; Sweigart, D. A. *Inorg. Chem.* **1985**, *24*, 296. (f) Byers, W.; Cossham, J. A.; Edwards, J. O.; Gordon, A. T.; Jones, J. G.; Kenny, E. T. P.; Mahmood, A.; McKnight, J.; Sweigart, D. A.; Tondreau, G. A.; Wright, T. *Inorg. Chem.* **1986**, *25*, 4767.

(23) Asher, S. A.; Adams, M. L.; Schuster, T. M. *Biochemistry* **1981**, *20*, 3339.

(24) Perutz, M. F. *Annu. Rev. Biochem.* **1979**, *48*, 327.